npj | vaccines

Article

Published in partnership with the Sealy Institute for Vaccine Sciences

https://doi.org/10.1038/s41541-025-01149-2

A *Plasmodium* LARC GAP provides preerythrocytic, stage and species transcending protection in mice

Raksha Devi [1,2], Rohini Nandi [1,2] & Satish Mishra [1,2]

Malonyl-CoA-acyl carrier protein transacylase (MCAT) catalyzes the transfer of a malonyl moiety from malonyl–CoA to acyl carrier protein during the initiation step of type II fatty acid synthesis (FASII). The *Plasmodium* FASII pathway was found to be essential for late liver-stage development in rodent malaria parasites. Here, we generated a novel genetically attenuated parasite (GAP) by disrupting *Plasmodium* MCAT. Deleting MCAT in rodent malaria parasites did not affect asexual blood-stage propagation and mosquito-stage development. MCAT KO sporozoites failed to initiate blood-stage infection in mice. Hepatic MCAT KO parasites showed impaired nuclear division and apicoplast biogenesis. This led to a defect in hepatic merozoite formation and attenuation of parasites during late liver stages. Vaccination of mice with MCAT KO sporozoites exhibited sterilizing immunity against homologous and heterologous species challenge. Further, MCAT KO-immunized mice were able to clear blood stage infection after iRBCs challenge. These findings highlight that late-liver arresting MCAT KO sporozoite is a promising GAP vaccine candidate for inducing pre-erythrocytic, stage, and species-transcending protection in mice.

Malaria continues to be a significant global health concern caused by an obligate intracellular protozoan parasite of the genus *Plasmodium*. According to the WHO Report 2024, there were 263 million malaria cases and 0.59 million deaths in 2023, with approximately 94% of these malaria cases occurring in sub-Saharan Africa[1]. Currently, malaria control programs aim to eliminate this deadly but preventable disease. However, the emergence of resistance against frontline antimalarials threatens advances in malaria control[2–4]. To accelerate the elimination of malaria, the development of a range of new and more effective solutions is urgently needed. RTS,S/AS01 and R21/Matrix-M are the two subunit vaccines recommended by WHO for use in Africa. Both vaccines elicit antibody responses against *Plasmodium falciparum* circumsporozoite protein (CSP)[5]. However, a key limitation of this type of vaccine is the lack of an efficient and durable immune response[6].

Compared with subunit vaccines, whole-sporozoite (WSp) vaccines induce greater antigenic breadth responses[7]. Three WSp vaccine approaches include radiation-attenuated sporozoites (RASs), genetically attenuated parasites (GAPs), and chemoprophylaxis and sporozoites (CPSs). RASs are metabolically active parasites that infect hepatocytes but arrest early in liver stage development and do not replicate their DNA[8,9]. Vaccination with PfSPZ RAS has provided 12–14 months of protection since the last immunization in malaria-naïve individuals[10]. CPS WSp is another type of vaccination in which sporozoites are given in combination with antimalarial agents, and it offers increased protection at lower doses than the RAS does[11,12]. However, the protective efficacy of CPS wanes rapidly over time, and questions of intrinsic safety and feasibility remain a concern at higher immunization dosages[13,14]. GAPs lack genes essential for liver stage development and have proven to be highly effective and provide much control over their safety and efficacy[10,15,16]. GAPs either arrest early (early arresting replication deficient, EARD) or late (liver stage-arresting replication-competent, LARC) during liver stage development[10,15–21]. The few successfully generated PfEARD GAPs were PfGAP3KO (Pfp52/p36/sap1 KO)[22] and PfSPZ-GA1 (Pfb9/slarp KO)[23], which provided 50% and 12% vaccine efficacy, respectively, in controlled human malaria infections (CHMI). LARC GAPs offer better pre-erythrocytic immunity than EARD GAPs do by expressing late liver-stage antigens. In addition, LARC GAPs are also capable of providing stage-transcending immunity due to the expression of blood-stage overlapping antigens (Goswami et al., 2024; Richie et al., 2023).

In our group, we recently generated a Scd/Scot1 LARC GAP by dual gene deletion that was safe at very high doses of sporozoites. Scd/Scot1 GAP immunization induced greater and broader CD8 + T-cell responses and elicited stage-transcending immunity[16]. Two other LARC GAPs, GA2 and LARC2, with mutations in mei2 and mei2/lineup, respectively, have also been characterized in mice and are advancing into humans[24–27].

[1]Division of Molecular Microbiology and Immunology, CSIR-Central Drug Research Institute, Lucknow, 226031, India. [2]Academy of Scientific and Innovative Research (AcSIR), Ghaziabad, 201002, India. e-mail: satish.mishra@cdri.res.in

Immunization with PyLARC2 elicited robust humoral and cellular immune responses and conferred sterile immunity against infection[15]. Next, they generated KOs in *P. falciparum* and cryopreserved PfSPZ-LARC2 for safety, immunogenicity, and efficacy trials planned in the near future in malaria-exposed Africans[15]. Recently, it was demonstrated that single immunization with GA2 via mosquito bites can induce substantial protection against sporozoite challenge infection[27]. *P. falciparum* sporozoites can be easily produced in the laboratory, and several PfWSp-based vaccine candidates are being assessed in clinical trials[28]. In contrast, *P. vivax* WSp has not been developed because of the lack of a continuous in vitro culture system. The use of transgenic *P. berghei* parasites expressing Pf or Pv antigens offers a promising approach for WSp vaccination against *P. falciparum* or *P. vivax*. PfCSP-expressing Pb sporozoites (PbVac) have been used as a vaccine platform for human malaria both preclinically[29] and clinically[30]. Recently, a Pb parasite expressing the VK210 variant of PvCSP (PbViVac) was generated[31]. The immunization of mice with PbViVac sporozoites elicited an antibody response that recognized and bound to Pv sporozoites[31]. This novel vaccination approach can be employed to fight Pv malaria.

The type II fatty acid synthesis pathway is essential for late liver-stage development in rodent malaria parasites. FAS II mutants in *P. yoelii* are completely arrested in the late liver stage of development[32,33]. However, occasional breakthrough infections have been observed with FAS II mutants in *P. berghei*[34,35]. The FASII pathway involves nine different enzymes, with four important enzymes responsible for catalyzing the extension step: FabB/F, FabG, FabI, and FabZ[33]. The essentiality of the FASII pathway differs among different *Plasmodium* species. Targeted deletion of key enzymes of the FASII pathway, such as FabB/F, FabZ, and FabI in *P. yoelii* were found to be dispensable for the blood and mosquito stages but essential for late liver stage development[33]. Late liver-arresting FabB/F KO parasites have long been used in preclinical mouse models to compare the immune response to RAS and EARD[36,37]. Unlike *P. yoelii*, genetic knockout of FabI and FabB/F in *P. falciparum* resulted in loss of sporogony[38]. Malonyl-CoA-acyl carrier protein transacylase (MCAT) is a key enzyme in the FAS II pathway that catalyzes the transfer of a malonyl group from malonyl-CoA to the acyl carrier protein (ACP)[39]. The generated Malonyl-ACP serves as a substrate for enzymes involved in the downstream extension step of the FASII pathway. Studies have shown that the prepared recombinant PfMCAT without a leader sequence at its N-terminal sequence exhibits malonyl-coenzyme A:ACP transacylase activity[40].

In this study, we selected PbMCAT and found that it was expressed in the blood, sporozoite, and liver stages and localized to the apicoplast. Targeted deletion of PbMCAT did not affect blood or mosquito stages development but arrested the parasite in the late liver stage, with occasional breakthrough infections. PyMCAT KO parasites showed a similar phenotype, with complete late liver-stage arrest and no liver-to-blood-stage infection. Vaccination with MCAT KO parasites confers sterilizing immunity against sporozoite challenge and provides species- and stage-transcending protection. Thus, MCAT is another gene target for generating LARC GAP vaccines.

Results

*Pb*MCAT is expressed in blood schizonts, sporozoites and the liver stage and is localized to the apicoplast

To detect PbMCAT throughout the parasite life cycle, we endogenously tagged the gene with the 3XHA epitope (Supplementary Fig. S1A). Correct gene tagging was confirmed by diagnostic PCR (Supplementary Fig. S1B). The resulting PbMCAT-3XHA transgenic parasites completed their life cycle normally (Supplementary Fig. S1C and S1D). The expression of the PbMCAT-3XHA fusion protein in the transgenic parasites was verified via Western blot analysis. As predicted, Western blotting of schizonts revealed the correct size of the PbMCAT-3XHA fusion protein (Fig. 1A). Next, we monitored PbMCAT expression via indirect immunofluorescence (IFA) assays with anti-HA antibodies. PbMCAT-3XHA expression was detected in blood schizonts (Fig. 1B), salivary gland sporozoites (Fig. 1C), and liver stages (Fig. 1D). We observed single dot staining in salivary gland sporozoites that colocalized with the anti-ACP signal, indicative of apicoplast localization. Furthermore, we analyzed anti-HA and anti-ACP co-immunostained liver-stage parasites. The staining pattern revealed PbMCAT localization in the apicoplast. Taken together, the expression and localization data indicate that PbMCAT is expressed in all stages of the parasite and is localized to the apicoplast.

Plasmodium MCAT is not required for blood-stage growth and mosquito stage development

To understand the importance of *Plasmodium* MCAT, we disrupted the gene via double cross-over homologous recombination (Supplementary Fig. S2A). Recombination enables the substitution of the MCAT ORF with GFP and hDHFR:yFCU cassette and successful replacement of the gene was confirmed by observing GFP-expressing parasites (Supplementary Figure S2B). Two clonal lines were obtained by limiting dilution of the parasites. The correct site-specific integration of the targeting cassette and the absence of the ORF were confirmed by diagnostic PCR (Supplementary Fig. S2C). To check the specificity of the phenotype, the PbMCAT complemented parasite line was generated by reintroducing the gene at the same locus (Supplementary Fig. S2D). The restoration of the locus was confirmed by diagnostic PCR (Supplementary Fig. S2E). The growth of PbMCAT KO

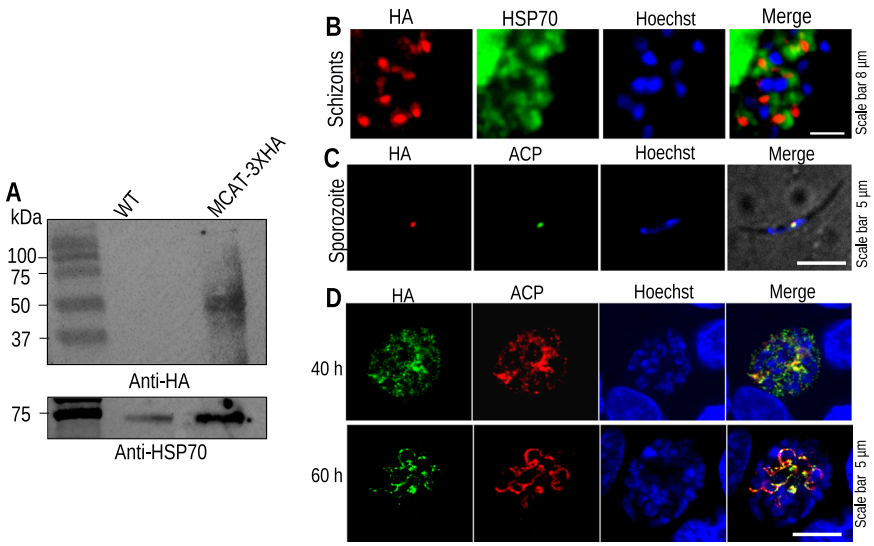

Fig. 1 | Expression and localization of PbMCAT during the parasite life cycle. A Western blot confirmation of PbMCAT-3XHA expression in blood-stage schizonts. Probing with an anti-HA antibody revealed a ~47 kDa PbMCAT-3XHA fusion protein. No bands were detected with the WT parasite lysate. The blot was stripped and reprobed with an anti-HSP70 antibody, which recognized the band in both WT and PbMCAT-3XHA parasite lysates. **B** PbMCAT-3XHA blood-stage schizonts were immunostained with anti-HA and anti-HSP70 antibodies. **C** Salivary gland sporozoites were immunostained with anti-HA and anti-ACP antibodies. **D** Coimmunostaining of fixed, PbMCAT-3XHA sporozoite-infected HepG2 cells at 40 and 60 hpi with anti-HA and anti-ACP antibodies. Nuclei were stained with Hoechst. Anti-HA signal overlaps with the apicoplast signal.

Table 1 | Infectivity of PbMCAT KO sporozoites in C57BL/6, BALB/c and Swiss albino mice

Exp.	Mice	Parasite	Number of sporozoites inoculated	Mice positive/Mice inoculated	Prepatent period (days)
1	C57BL/6	WT GFP	5000	5/5	3
		PbMCAT KO c1	5000	2/5	9
		PbMCAT KO c2	5000	1/5	9
		PbMCAT Comp	5000	5/5	3
2	C57BL/6	WT GFP	5000	5/5	3
		PbMCAT KO c1	5000	0/5	NA
		PbMCAT KO c2	5000	1/5	9
3	C57BL/6	WT GFP	5000	5/5	3
		PbMCAT KO c1	5000	1/5	9
		PbMCAT KO c1	10,000	1/5	9
		PbMCAT KO c1	20,000	2/13	8.5
		PbMCAT KO c1	50,000	1/5	7
4	BALB/c	WT GFP	20,000	3/3	3
		PbMCAT KO c1	100,000	0/5	NA
	Swiss albino	WT GFP	20,000	3/3	3
		PbMCAT KO c1	100,000	0/5	NA
5	BALB/c	WT GFP	20,000	3/3	3
		PbMCAT KO c1	100,000	0/5	NA
	Swiss albino	WT GFP	20,000	3/3	3
		PbMCAT KO c1	100,000	0/5	NA
Exp.		**Parasites**	**Number of mosquitoes/mice**	**Mice positive/Mice infected**	**Pre-patent period (days)**
Mosquito bite	C57BL/6	WT GFP	20	5/5	4
		PbMCAT KO c1	20	0/5	NA
		PbMCAT KO c2	20	0/5	NA

parasites was then evaluated, which was comparable to that of WT GFP parasites. (Supplementary Figure S2F). To determine the PbMCAT KO phenotype in the mosquito and liver stages, we transmitted the parasites to the mosquitoes by allowing them to probe for blood meal in infected mice. We found that ookinete, oocyst, and midgut sporozoite development was normal in PbMCAT KO parasites (Supplementary Fig. S3A-F). Next, we evaluated the sporozoite numbers in the salivary glands of PbMCAT KO parasites, which were comparable to those of WT GFP parasites (Supplementary Fig. S3G-H). These findings demonstrate that PbMCAT is dispensable for blood and mosquito stage development.

PbMCAT knockout sporozoites exhibit occasional breakthrough infection in C57BL/6 mice

To determine the effect of PbMCAT deletion during liver stage development, PbMCAT KO, WT GFP and PbMCAT complemented (PbMCAT comp) salivary gland sporozoites were injected intravenously into groups of C57BL/6 mice. Another group of mice was inoculated with sporozoites through mosquito bites. The appearance of parasites in the blood was determined via examination of Giemsa-stained blood smears. All the mice inoculated with WT GFP or PbMCAT complemented sporozoites developed blood-stage infection within a normal prepatent period. Moreover, PbMCAT KO sporozoites either completely failed to develop a blood-stage infection or exhibited occasional breakthrough infection with delayed patency (Table 1). Compared with BALB/c mice, C57BL6 mice are highly susceptible to *P. berghei* sporozoite infections[41]. Next, we tested PbMCAT KO sporozoite infection in BALB/c and Swiss albino mice, which resulted in complete attenuation at higher sporozoite doses (100,000) compared with the incomplete attenuation phenotype in C57BL/6 mice (Table 1). To determine the stage-specific defect, we investigated the invasion ability of the PbMCAT KO sporozoites. We found that PbMCAT KO sporozoites invaded hepatocytes normally. Next, we quantified the parasite biomass in the liver after sporozoite inoculation. We found that parasite biomass was comparable in PbMCAT KO and WT GFP-infected mice livers harvested at 40 hpi. However, there was a significant decrease in the parasite biomass in PbMCAT KO-infected livers at 55 hpi (Fig. 2). Taken together, these results demonstrate that PbMCAT is critical for late liver stage development.

Late arresting PbMCAT KO parasites display impaired apicoplast branching and cannot form hepatic merozoites

To further investigate the observed defects in PbMCAT KO liver stage development, HepG2 cells were infected with PbMCAT KO sporozoites. The cultures were harvested at different time points and fixed with 4% paraformaldehyde (PFA). IFA with an anti-UIS4 antibody revealed similar growth patterns in WT GFP and PbMCAT KO exoerythrocytic forms (EEFs) (Fig. 3A). We enumerated the number and size of EEFs at 40 and 55 hpi and detected no difference between WT GFP and PbMCAT KO parasites (Fig. 3B, C). Next, we immunostained EEFs harvested at 65 hpi with anti-ACP or anti-MSP1 antibodies to visualize apicoplast or merozoite development, respectively. We found impaired apicoplast branching in PbMCAT KO parasites that failed to form merozoites (Fig. 4A, B). At 65 hpi, differences in DNA segregation were evident between PbMCAT KO and WT GFP parasites (Fig. 4C). Next, we observed the culture supernatant to form detached cells (merosomes). We detected detached cells in the WT GFP-infected culture but not in the PbMCAT KO-infected culture. To quantify the number of detached cells, the culture supernatants were collected and counted via a hemocytometer (Fig. 4D). We did not observe detached cells in PbMCAT KO; hence, the same amount of culture supernatant was injected into Swiss mice to assess infectivity. WT GFP-injected mice developed blood-stage infection, whereas the PbMCAT KO-injected group remained negative until the observation period of 20 days (Table 2). Together, these results demonstrate that PbMCAT plays a role in apicoplast biogenesis and hepatic merozoite formation.

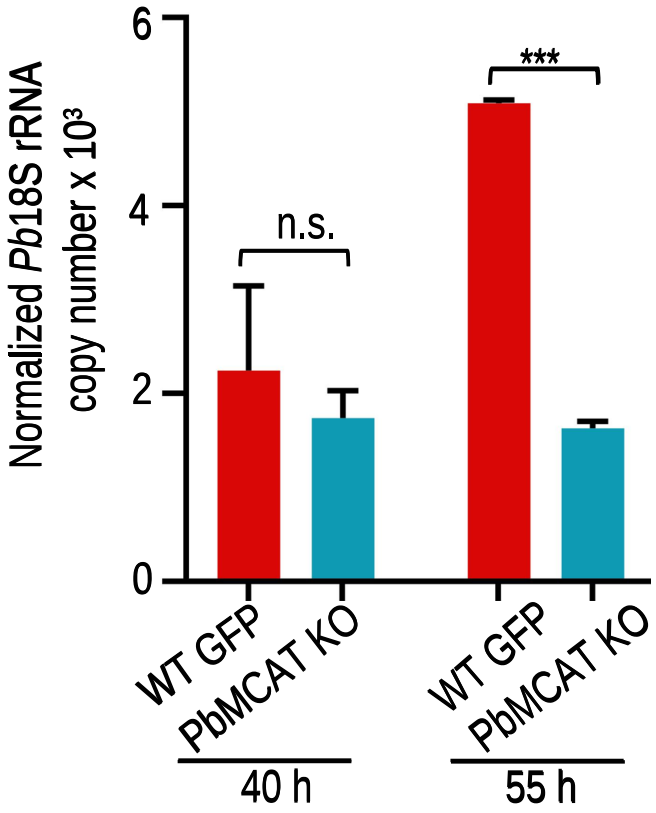

Fig. 2 | PbMCAT KO parasites exhibit defects in the late liver stage development. We infected the mice with 5×10^3 PbMCAT KO sporozoites, and livers were harvested at 40 and 55 hpi. RNA was extracted, cDNA was synthesized, and the parasite burden was quantified by measuring Pb18s rRNA levels via real-time PCR. There was no difference in parasite burden at 40 hpi ($P = 0.6476$), but it was significantly decreased in PbMCAT KO parasites than in WT GFP parasites at 55 hpi (***$P = 0.0006$). The data are shown as mean ± SEM of two independent experiments. $n = 5$ mice per group. Statistical significance was measured using the Student's *t*-test.

PyMCAT KO parasites show complete attenuation in the liver

The attenuation level of the same gene KO differed between *P. yoelii* and *P. berghei*. FAS II mutants were completely attenuated in *P. yoelii* but showed occasional breakthrough infections in *P. berghei*[33,34]. However, no reports have compared the attenuation levels of KO parasites in these two rodent malaria species. Owing to the occasional breakthrough infection observed with the PbMCAT KO parasite, we created its KO in *P. yoelii*. Like the PbMCAT KO construct, we generated the PyMCAT targeting construct by cloning two fragments in the pBC-GFP-hDHFR vector (Supplementary Fig. S4A). Integration of the targeting cassette was confirmed by observing GFP-expressing parasites (Supplementary Fig. S4B), and diagnostic PCR confirmed site-specific integration (Supplementary Fig. S4C). Consistent with the PbMCAT KO phenotype, PyMCAT KO parasites exhibited similar blood growth and mosquito stage development (Supplementary Fig. S4D-F). These observations confirm the dispensability of MCAT for blood and mosquito stage development in rodent malaria parasites.

To further investigate the infectivity of PyMCAT KO sporozoites, BALB/C mice were inoculated with 5×10^3 to 5×10^5 sporozoites. The appearance of parasites in the blood was observed by making Giemsa-stained blood smears. All the mice inoculated with PyWT sporozoites became patent on day 3 post-infection, whereas the KO-inoculated mice did not develop blood-stage infection until the observation period of 20 days (Table 3).

Immunization with MCAT KO parasites protects against infectious sporozoite challenge

To determine whether immunization with MCAT KO sporozoites protects against infectious sporozoite challenge, C57BL/6, and BALB/c mice were immunized intravenously (i.v.) thrice with 20,000 PbMCAT and PyMCAT KO sporozoites, respectively, at intervals of two weeks (Fig. 5A, E). The control mice were mock immunized with an equivalent volume of uninfected mosquito salivary gland debris (SGD). Another group included naïve mice that did not receive any immunogen. Ten days after the last immunization, the mice were challenged with 5000 PbWT or 10,000 PyWT infectious sporozoites. Another group of mice that were immunized with PbMCAT or PyMCAT KO sporozoites was challenged with 5000–10,000 PbGFP-luciferase-expressing infectious sporozoites. The parasite load in the liver was measured by quantifying bioluminescence using an in vivo

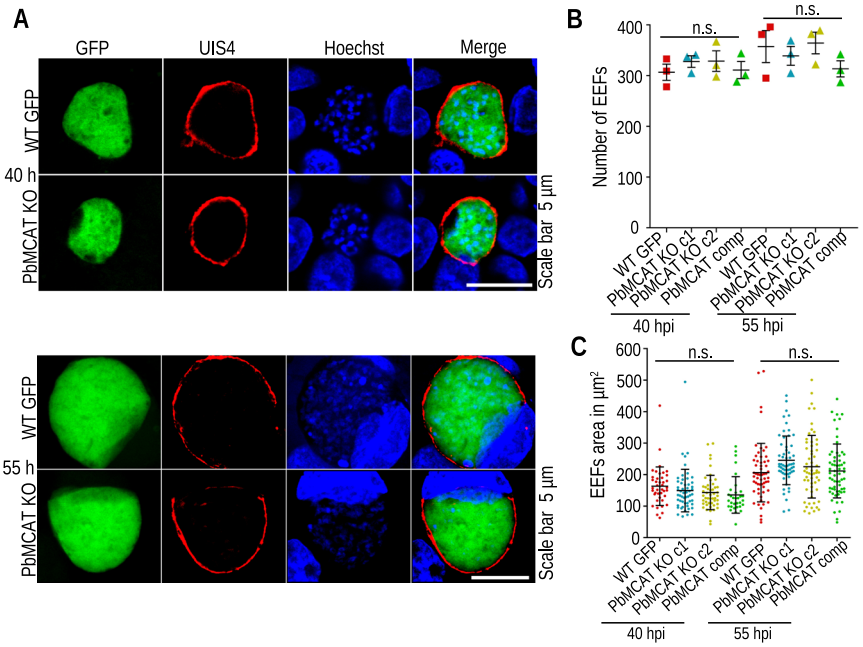

Fig. 3 | PbMCAT is not required for parasite growth in the liver. A HepG2 cultures were infected with WT GFP and PbMCAT KO sporozoites and fixed at the indicated time points. Parasites were stained with an anti-UIS4 antibody, and nuclei were stained with Hoechst. Visually, the growth of EEFs was comparable in WT GFP and PbMCAT KO parasites. **B** The number of EEFs was counted under a fluorescence microscope. The numbers were similar between WT GFP and PbMCAT KO parasites at 40 ($P = 0.7094$) and 55 hpi ($P = 0.4348$). The counts from three independent experiments are presented as Mean ± SEMs performed in duplicate. **C** Images were acquired using a fluorescence microscope to determine the EEF area, and the area was measured via Nikon NIS elements BR imaging software. The EEF area was comparable between PbMCAT KO and WT GFP at 40 ($P = 0.2434$) and 55 hpi ($P = 0.1671$). Data from 41, 54, 48 and 32 (40 h) and 58, 59, 59 and 62 (55 h) EEFs of WT, PbMCAT KO c1, PbMCAT KO c2 and PbMCAT complemented parasites are shown. The data from three independent experiments are presented as mean ± SEM performed in duplicate. Statistical significance was measured using the Student's *t*-test.

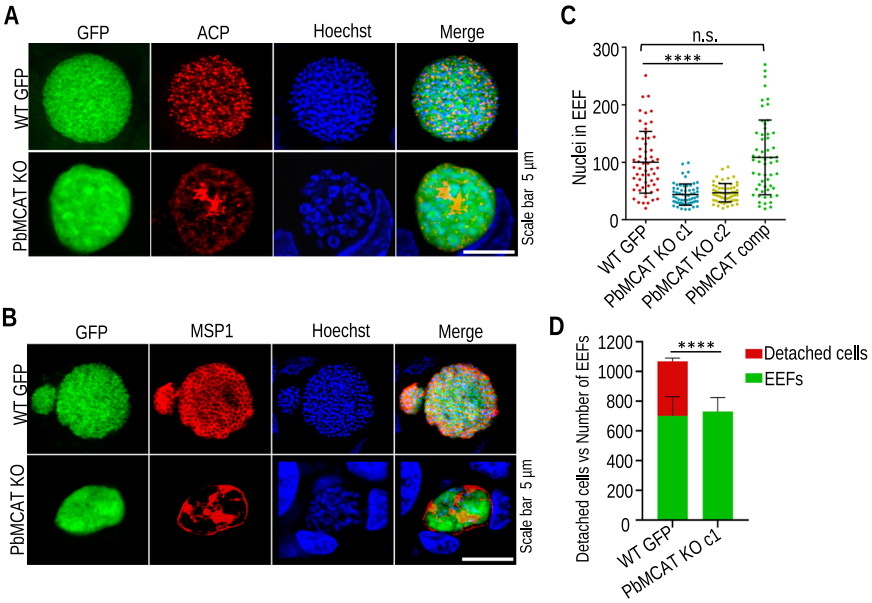

Fig. 4 | PbMCAT KO parasites exhibit impaired late liver stage development. A Infected HepG2 cultures harvested at 65 hpi were immunostained with an anti-ACP antibody. PbMCAT KO parasites show impaired apicoplast branching. **B** Infected HepG2 cultures harvested at 65 hpi were immunostained with an anti-MSP1 antibody. PbMCAT KO parasites do not show MSP1 staining and fail to form merozoites. **C** Infected cultures harvested at 65 hpi were stained with Hoechst, and the nuclei were counted. The data were pooled from three independent experiments and are presented as the mean ± SEM. 59, 60, 60 and 57 EEFs of WT GFP, PbMCAT KO c1, PbMCAT KO c2 and PbMCAT comp, respectively, were analyzed. The number of nuclei was significantly decreased in PbMCAT KO parasites (****$P = < 0.0001$, one-way ANOVA). **D** Detached cells were collected from infected HepG2 cultures at 65 hpi and counted using a hemocytometer. The data are presented as the number of detached cells produced from the total number of EEFs. No detached cells were observed in PbMCAT KO parasites despite producing comparable EEFs with WT GFP (****$P < 0.0001$), Student's t-test). Data from three independent experiments is shown as mean ± SEM.

Table 2 | Infectivity of detached cells in Swiss mice

Parasite	Number of Detached cells injected	Mice positive/ Mice injected	Prepatent period (days)
WT GFP	10	5/5	4
PbMCAT KO c1	Supernatant	0/5	NA
PbMCAT KO c2	Supernatant	0/5	NA

Table 3 | Infectivity of PyMCAT KO sporozoites in BALB/c mice

Experiment	Parasite	Number of sporozoites inoculated	Mice positive/ Mice inoculated	Prepatent period(day)
1	PyWT	5000	5/5	3
	PyMCAT KO	5000	0/5	NA
2	PyWT	5000	5/5	3
	PyMCAT KO	200,000	0/5	NA
3	PyWT	10,000	3/3	3
	PyMCAT KO	500,000	0/5	NA
4	PyWT	10,000	3/3	3
	PyMCAT KO	500,000	0/5	NA

imaging system (IVIS) at 42–44 hpi. All SGD-immunized mice showed a strong luciferase signal, whereas no bioluminescence was observed in MCAT KO-immunized mice (Fig. 5B, C, F and G). Next, all the mice challenged with homologous or heterologous parasites were observed for blood-stage infection by making Giemsa-stained blood smears. All the control mice became patent after the challenge. In contrast, KO-immunized mice remained negative throughout the observation period and were thus protected against sporozoite challenge (Figs. 5D, H and I). These results demonstrate that immunization with MCAT KO parasites provides sterile and species-transcending protection.

Immunization with LARC GAP elicits long-lasting and stage-transcending protection

Next, we investigated durability and stage-transcending protection in BALB/c mice immunized with PyMCAT KO sporozoites (LARC GAP). Groups of BALB/c mice were intravenously immunized three times with 50,000 PyMCAT KO sporozoites at intervals of one month (Fig. 6A). The control mice were mock immunized with SGD, and another group of naïve mice did not receive any immunogen. All three groups of mice were then challenged with 10,000 *P. yoelii* infectious sporozoites on day 70. All the control mice developed blood-stage infection, whereas PyMCAT KO-immunized mice were completely protected against challenge (Fig. 6B). We next investigated durability by rechallenging the mice with 10,000 PyWT sporozoites on day 250. Eight of the ten mice were completely protected against the challenge. Mice that were blood-stage positive displayed delayed patency (Fig. 6C). To investigate the ability of LARC GAP to elicit cross-stage immunity, another group of BALB/c mice were challenged intravenously with 5000 *P. yoelii* iRBCs on day 70. The control mice developed blood-stage parasitemia that increased over time and were euthanized according to the animal protocol 7 days after the challenge. LARC GAP-immunized mice showed reduced parasitemia, which was cleared 13 days after iRBC challenge (Fig. 6D). We next decreased the number of immunization dosages to assess the impact on protective efficacy. To this end, groups of BALB/c mice were immunized twice, either intravenously (i.v.) or intramuscularly (i.m.), with 50,000 PyMCAT KO sporozoites at intervals of 1 month (Fig. 6E). Thirty days after the last immunization, the mice were i.v. challenged with 10,000 *P. yoelii* infectious sporozoites. All the control mice developed blood-stage infection, whereas PyMCAT KO-immunized mice via the i.v. route were completely protected against challenge (Fig. 6F). Nine of the ten mice immunized with PyMCAT KO sporozoites via the i.m. route were protected against infection (Fig. 6G). Furthermore, we assessed protection after a single dose was administered via the i.v. or i.m. route. BALB/c mice were immunized with 50,000 PyMCAT KO sporozoites and challenged with 10,000 *P. yoelii* infectious sporozoites thirty days after the immunization (Fig. 6H). All the control mice developed blood-stage infections, whereas PyMCAT KO-immunized mice via the i.v. route were completely protected against challenge (Fig. 6I). Fifty percent of the mice immunized with PyMCAT KO sporozoites via the i.m. route were protected against infection (Fig. 6J). These results demonstrate that immunization

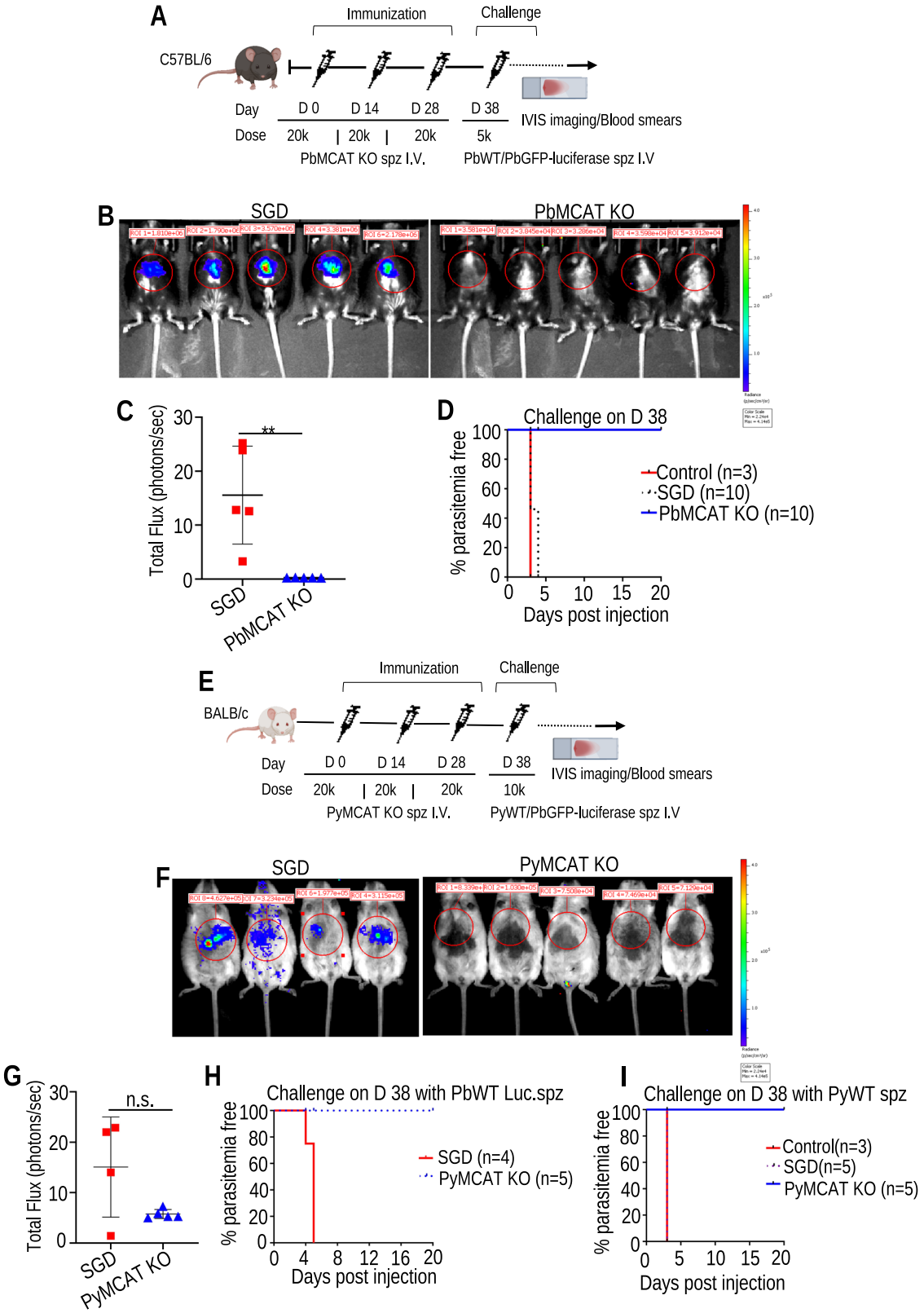

with LARC GAP elicits long-lasting and stage-transcending protection and that different administration routes can be used for protective vaccination.

LARC GAP immune sera recognize different stages of parasites and inhibit sporozoite infection

Next, we evaluated the humoral immunity generated by PbLARC GAP. To investigate the antibody response, sera were collected from naïve or immunized C57BL/6 mice and pooled (Fig. 7A). For comparison with PbEA-GAP, sera from a previous study were used[16]. We next performed IFA with immune sera against different stages of the parasites. PbLARC GAP sera recognized sporozoites, liver, and blood-stage parasites. EA-GAP sera recognized sporozoites and liver but did not recognize blood-stage parasites (Fig. 7B–D). To determine the effect of the sera on sporozoite infection, sporozoites were incubated with the sera and then added to the HepG2

Fig. 5 | Immunization with LARC GAP prevents sporozoite infection and provides species-transcending protection. **A** Groups of C57BL/6 mice were intravenously (i.v.) immunized and challenged, as shown in the schematic. **B** Luciferase signals were detected in C57BL/6 mice using an in vivo imaging system after challenge with PbGFP-luciferase sporozoites. No signals were detected in the mice immunized with PbMCAT KO parasites. **C** Luciferase signals were quantified and are presented as total flux/second. There was a significant difference in luciferase signals between SGD- and PbMCAT KO-immunized mice (**$P = 0.0055$, Student's t test). The data are presented as mean ± SD. **D** The survival curve shows the percentage of C57BL/6 mice that were negative for parasites in a Giemsa-stained blood smear during the observation period of 20 days after sporozoite challenge. n = number of mice. A significant difference was observed between the control and immunized groups (****$p < 0.0001$, log-rank Mantel–Cox test). **E** Groups of BALB/c mice were intravenously immunized and challenged as shown in the schematic. **F** Detection of luciferase signals in BALB/c mice after challenge with PbGFP-luciferase sporozoites. **G** Luciferase signals were not detected in mice immunized with PyMCAT KO parasites. However, the difference was statistically insignificant due to masking of a signal in a group scan of the mice ($P = 0.0713$, Student's t-test). The data are presented as the mean ± SD. **H**, **I** The survival curve shows the percentage of BALB/c mice that were negative for the parasites in a Giemsa-stained blood smear either challenged with PbGFP-luciferase or PyWT parasites and observed up to 20 days after the sporozoite challenge. n = number of mice. A significant difference was observed between the control and immunized groups in both PbGFP-luciferase challenged (***$P = 0.0002$) and PyWT challenged (****$p < 0.0005$) mice groups. Statistical analysis was done using the log-rank Mantel-Cox test.

culture. We observed a significant reduction in the EEFs produced by EA-GAP and LARC GAP sera-incubated sporozoites compared with those produced by preimmune serum-incubated sporozoites (Fig. 7E). These results demonstrate that LARC GAP-immunized mice generate robust pre-erythrocytic and blood-stage humoral immune responses.

Discussion

Plasmodium possesses its own FASII pathway, which is localized to the apicoplast[42]. FASII pathway elongation enzymes were found to be dispensable for the blood and mosquito stages but essential for the late liver stage development in rodent malaria parasites[33,34]. FASII pathway genes fabI and fabB/F mutants were generated in *P. falciparum* to immunize humans. However, these mutants were found to be essential for sporozoite development in the mosquito midgut, raising concerns about the generation of FASII elongation gene mutants as GAP vaccines[38]. Here, we report the role of the enzyme MCAT that catalyzes the transfer of a malonyl group from malonyl-CoA to ACP before the FASII pathway enters the elongation step. Disruption of MCAT in the rodent malaria parasites *P. berghei* and *P. yoelii* resulted in phenotypes similar to those of the other FASII gene mutants. However, the attenuation level of MCAT KO differed between *P. yoelii* and *P. berghei*. PyMCAT KO parasites were completely attenuated with an inoculum as high as 5×10^5 sporozoites, but PbMCAT KO parasites in C57BL/6 mice presented occasional breakthrough infections. Similarly, FASII mutants analyzed previously were completely attenuated in *P. yoelii* but not in *P. berghei*[33,34]. Interestingly, Pyp52/p36[43] or Pyfabb/f deficient parasites[33] were completely arrested in BALB/c mice and failed to initiate blood-stage infections even at high sporozoite inoculation doses. In *P. falciparum*, p52/p36-based GAP showed comparable attenuation[44]. However, disruption of the same genes in *P. berghei* resulted in incompletely attenuated GAP[35]. Surprisingly, another p52/p36 double-gene deletion line generated in *P. falciparum*[35] produced replicating liver stages, contrary to previous reports of severe intrahepatocytic growth defects[44]. Overall, these reports indicate that the deletion of candidate genes across different species can lead to different phenotypes. It was also found that mutant parasites behave differently in different hosts. In fact, *P. berghei* p52/p36 mutant parasites exhibited different attenuation levels in BALB/c and C57BL/6 mice. Compared with occasional breakthrough blood infections in C57BL/6, no breakthrough blood infections were observed in BALB/c mice[35]. Another example is the deletion of PDH-E1α, which generated completely attenuated *P. yoelii* parasites compared with the incompletely attenuated *P. berghei* ortholog[45]. Therefore, we tested PbMCAT KO infection in BALB/c and Swiss albino mice and, interestingly, found complete attenuation compared with the incomplete attenuation phenotype in C57BL/6 mice. Therefore, we propose stringent screening criteria to assess the adequacy of sporozoite attenuation in multiple rodent malaria parasites in different mouse strains before advancing into further clinical development and studies in humans.

The difference in the attenuation level between the two rodent malaria species might be due to a difference in the dependence on FASII for successful liver-stage development. Alternatively, these findings reflect differences in the virulence of the two rodent malaria parasites. *P. berghei* ANKA parasites produce severe lethal infections compared with *P. yoelii* 17XNL infections, which are nonlethal and can be cleared by host immune responses[34]. Another reason for differences in attenuation among *Plasmodium* mutants may also be due to differences in intracellular survival of attenuated sporozoites in different hosts. Interestingly, our observation of PbMCAT KO sporozoites in different hosts suggest that sporozoite attenuation is not only dependent on *Plasmodium* species but also influenced by host factors. This study highlights the potential of *P. berghei* / C57BL/6 mouse models for preclinical testing of GAPs. A *P. berghei* mutant completely attenuated in C57BL/6 mice may have a better chance of success in *P. falciparum* than *P. yoelii* in BALB/c or Swiss mice. The complete attenuation phenotype of MCAT GAP in *P. falciparum* can be tested by its inability to form viable hepatic merozoites using the humanized liver mouse of infection as previously described[15,22,25].

FASII elongation step enzymes were found to be unsuitable for generating GAP in *P. falciparum* because of their role in sporozoite formation[38]. Future work might determine whether the deletion of MCAT in *P. falciparum* affects sporozoite formation in the mosquito midgut. Our fully late liver-arrested PyMCAT GAP warrants further investigation as a GAP in *P. falciparum*. LARC GAPs constitute a promising approach for developing a safe and efficacious WSp vaccine that induces pre-erythrocytic and stage-transcending protection. Depending on gene function, GAPs can be customized to arrest late during liver stage development[46]. LARC GAPs have an advantage over RASs because knockout parasites are clonal lines that do not rely on external technical variables such as the radiation dosage and their consistency in attenuation in different batches of sporozoites[15,16]. The PfLARC2 candidate represents a promising future for WSpz malaria vaccines[15,28,47,48], which holds great promise in the global fight against malaria. PfLARC2 was generated by double deletion of the Mei2/LINUP genes because individually, Mei2 and LINUP KO parasites showed rare breakthrough infections[24,25,49,50]. However, our quest for new candidates should continue until LARC2 shows success in malaria-naïve healthy adults and in malaria-endemic settings where prolonged exposure to genetically diverse *P. falciparum* infections may impact vaccine performance. In fact, we have witnessed that irradiated sporozoites or GAP vaccination yielded lower protection in endemic individuals[51] than in malaria naïve volunteers[52]. On the basis of our data on PyMCAT KO, we project PyMCAT as a GAP vaccine for inclusion in future double- or triple-KO parasites with Scd/Scot1[16]. The protective efficacy and favorable safety profile of PyMCAT GAP are highly encouraging. The safety profile of PbMCAT GAP in BALB/c and Swiss albino mice amplifies our enthusiasm, as all the mice were negative for blood-stage infection when inoculated with high doses of sporozoites. LARC2 does not express MSP1 in the infected liver. However, it protects against blood-stage infection. Although MCAT or Scd/Scot1 KO parasites do not form hepatic merozoites, they partially express MSP1. Like LARC2, we achieved 100% protection against blood-stage challenge. A direct comparison of protection correlates is needed to prioritize a GAP vaccine. One important question in the future is, therefore, which GAP vaccines should be prioritized for future development. In this context, the

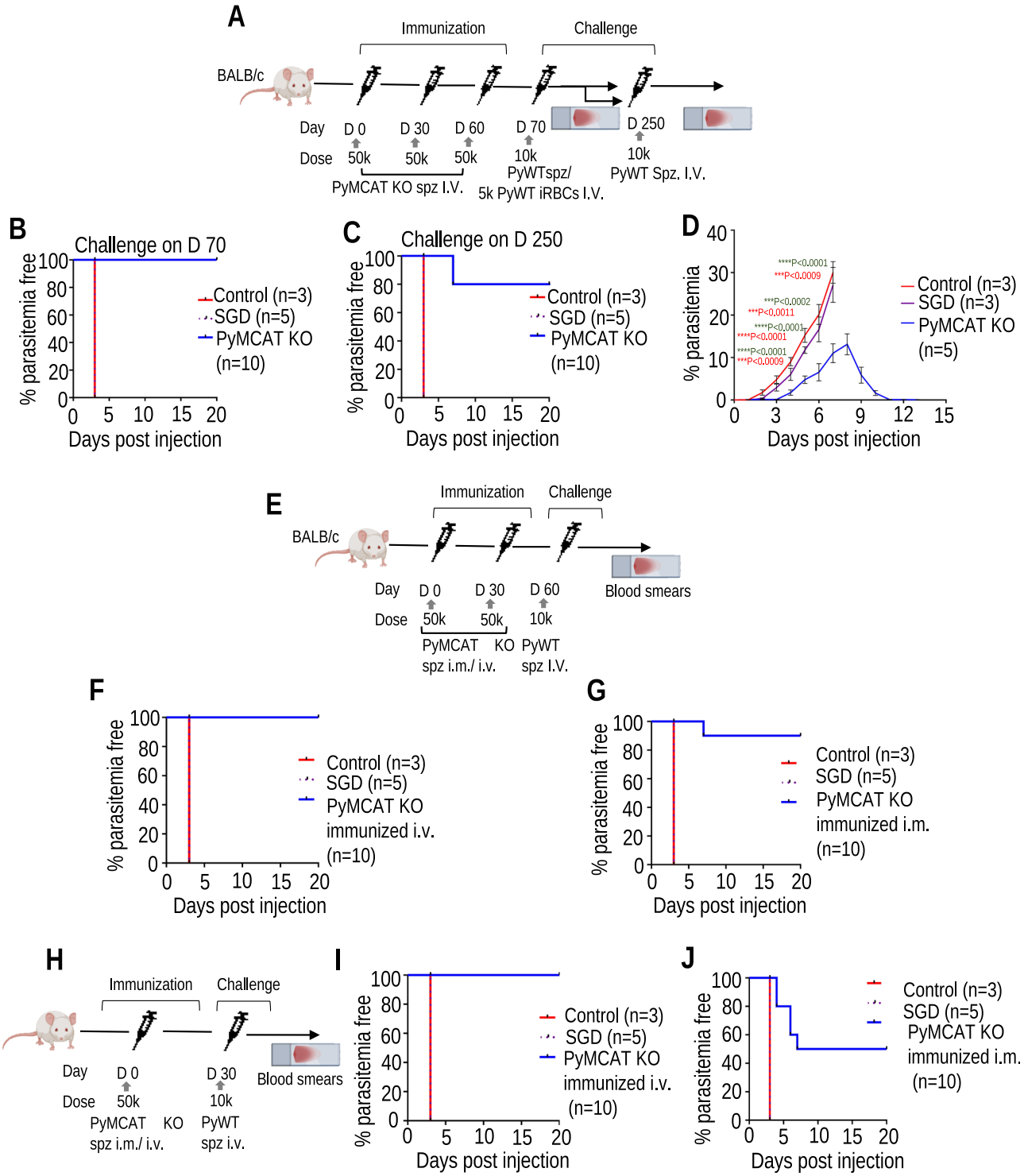

results of the ongoing clinical evaluation of Pf-LARC2 are highly anticipated. We believe that the reality of WSpz malaria vaccination is indeed possible, and this goal was achieved by continuously identifying novel candidates for generating GAP. Similarly, our quest to identify novel GAP vaccine candidates continues to improve the existing ones.

The expression data revealed that MCAT is expressed in the blood, sporozoite, and liver stages. Like FASII pathway elongation enzymes, MCAT is essential only for *Plasmodium* late liver stage development but not for the blood and mosquito stages. Thus, in all other life cycle stages, the parasite can scavenge fatty acids from the host. The way in which the parasite utilizes lipids from the mosquito midgut is not clear, but it has been clearly shown that parasites scavenge fatty acids from the host serum during the blood stage growth[53,54]. The functional significance of MCAT expression in sporozoites is unclear; nevertheless, the enzyme is not important for sporozoite formation. This is not surprising because several genes upregulated in infectious sporozoites (UISs) are dispensable in sporozoites but essential in liver stage development[18,43,55–58].

The FASII pathway for de novo fatty acid synthesis occurs in the apicoplast. *Plasmodium* can scavenge lipids from its host and also utilize its own de novo fatty acid synthesis[59]. Deletion of genes encoding FASII

Fig. 6 | Immunization with PyMCAT KO sporozoites confers durable and stage-transcending protection. A Groups of BALB/c mice were intravenously immunized and challenged, as shown in the schematic. **B** The survival curve shows the percentage of BALB/c mice that were negative for the parasites in a Giemsa-stained blood smear, challenged with PyWT parasites on day 70, and observed up to 20 days after the sporozoite challenge. A significant difference was observed between the control and immunized groups (***$P < 0.0001$). **C** Mice protected after challenge with sporozoites on day 70 were rechallenged on day 250. All control mice became blood-stage positive, whereas 80% of PyMCAT KO immunized mice were protected. A significant difference was observed between control and KO-immunized mice (****$P = < 0.0001$). **D** Stage transcending protection in BALB/c mice immunized with PyMCAT KO sporozoites followed by challenge with 5×10^3 PyWT iRBCs. All Naïve, SGD- and PyMCAT KO-immunized mice developed parasitemia, which grew exponentially in the naïve and SGD-immunized mice. However, parasitemia in PyMCAT KO-immunized mice started decreasing after reaching a point that was cleared 13 days after the challenge. Data is presented as mean ± SD. Statistical analysis was performed using Student's *t*-test. *P* values of naïve vs PyMCAT KO and SGD vs PyMCAT KO are shown in green and red, respectively. **E** Groups of BALB/c mice were immunized twice, either i.v. or intramuscularly (i.m.), and challenged, as shown in the schematic. **F, G** The survival curve shows the percentage of BALB/c mice that were immunized twice, either i.v. or i.m., and were negative for the parasites in a Giemsa-stained blood smear and challenged with PyWT parasites on day 60. A significant difference was observed between the control and immunized groups (****$P < 0.0001$). **H** Groups of BALB/c mice were immunized once either i.v. or i.m. and challenged, as shown in the schematic. **I, J** The survival curve shows the percentage of BALB/c mice immunized once either i.v. or i.m. and negative for the parasites in a Giemsa-stained blood smear and challenged with PyWT parasites on day 30. A significant difference was observed between the control and immunized groups (****$P < 0.0001$). n = number of mice. Statistical analysis of survival curves was performed using the log-rank Mantel–Cox test.

elongation enzymes results in parasite arrest in the late liver stage development[33,34,60]. The parasite undergoes remarkable growth and development during the liver stage, increasing the cell mass ~10,000-fold and forming thousands of merozoites[61]. MCAT KO liver-stage parasites displayed aberrant organelle segregation and no merozoite formation. MCAT KO parasites also displayed a lack of merosome formation. Despite similarities in phenotype, PbMCAT KO parasites showed occasional breakthrough infections compared to completely arrested *P. yoelii* KO parasites. The exclusive role of MCAT in the liver stage is possibly due to the formation of thousands of hepatic merozoites for which the demand for lipids cannot be met by the host and the parasite switches to de novo synthesis. A further hypothesis is that the fatty acids are likely converted into the phospholipids necessary for the massive membrane expansion of the developing apicoplast[62].

We assessed the efficacy of MCAT GAP in mice. BALB/c mice were immunized once or twice via the i.v. route with PyMCAT GAP and challenged thirty days after the last immunization were completely protected. However, the protection was decreased when mice were immunized via the i.m. route. Three vaccination doses of 2×10^5 PbMCAT or PyMCAT GAPs in C57BL/6 or BALB/c mice, respectively, completely prevented parasite development in the liver and blood stages against infectious sporozoites challenge. We also showed that PyMCAT GAP immunized mice were protected against challenge with the heterologous species *P. berghei* sporozoite. The antigens eliciting immunity in the liver are unknown. Nevertheless, species-transcending protection indicates that the antigens expressed during the *Plasmodium* liver stage are possibly conserved across malaria parasite species[63]. We evaluated protection in PyMCAT GAP-immunized BALB/c mice receiving three doses of sporozoites at an interval of one month and demonstrated long-lasting and stage-transcending protection. Challenging mice 10 days after the last immunization provided 100% protection against sporozoites and iRBC challenge. Immunized mice were cleared and survived an iRBC challenge, indicating that LARC GAP expressed several blood-stage antigens[15,16]. Rechallenging mice after ~7 months provided 80% protection. We previously showed that the immune response in Scd/Scot1 GAP immunized mice wanes over 6 months. In agreement with previous reports[15], our data indicate that immunization with PyMCAT GAP provides long-lasting protection.

This study also highlights the superiority of LARC GAP over EA-GAP. Both GAPs elicited similar pre-erythrocytic immune responses. However, LARC GAP also induced a stage-transcending immune response. The development of MCAT KO-based LARC GAP in *P. falciparum* is highly possible. Several GAPs validated in preclinical studies were successful in human malaria parasites. However, clinical studies on *P. falciparum* LARC GAPs are essential for determining the fate of this LARC GAP. Few *P. falciparum* GAPs cause breakthrough infections at high doses of sporozoites[62]. The LARC GAP generated in this study can be combined with other LARC GAPs, such as Scd[64] or Scot1 KO[55] parasites, for complete attenuation if this leads to any breakthrough infection in humans. The protection of PyMCAT GAP immunized mice wanes over the course of 6 months. Hence, before the translation of PyMCAT GAP into a human malaria parasite, a detailed evaluation of T cell functionality is warranted. These studies can be used to rapidly investigate and prioritize PyMCAT GAP for subsequent human assessment. The essentiality of MCAT also indicates the development of an inhibitor against this enzyme. An inhibitor may be developed to kill liver-stage parasites and contribute to malaria elimination.

Methods

Mice

Animal experiments were performed at the animal facility of CSIR-Central Drug Research Institute, India. Six to eight-week-old female Swiss albino mice were used for the passage and transmission of parasites. C57BL/6 and BALB/c mice (6–8 weeks old) were used for *P. berghei* and *P. yoelii* sporozoite infection. All animal experiments were conducted following the approval of procedures from the Institutional Animal Ethics Committee at CSIR-Central Drug Research Institute, India (IAEC reference no: IAEC/2018/F-03, IAEC/2023/15 and IAEC/2025/33). Mice were kept under a 12 h light/dark cycle at a temperature of 23°C ± 2°C and 55 ± 10% relative humidity. Feed and water were provided ad libitum. Mice were sedated by intraperitoneal injection of 100–200 mg/kg and 5-16 mg/kg body weight of Ketamine and Xylazine, respectively. Infected mice were euthanized when they presented signs of severe discomfort from exposure to carbon dioxide.

Parasites, mosquitos and cell lines

Rodent malaria parasites *P. berghei* ANKA (MRA-311), *P. berghei* ANKA GFP (MRA-867 507 m6cl1) and *P. yoelii* 17XNL (MRA-593 1.1) were obtained from BEI Resources, USA. As previously described, *P. berghei* sporozoites were obtained by infecting female *Anophleles stephensi* mosquitoes[16]. *P. yoelii-infected* mosquitoes were kept in an environmental chamber at 25°C with 80% relative humidity. Parasite liver stage development was analyzed by infecting Human liver hepatocellular carcinoma (HepG2) cells as previously described[16].

Generation of MCAT KO and complemented parasite lines

PbMCAT (PBANKA_1410500) was disrupted by double-crossover (DCO) homologous recombination. For DCO, two fragments, F1 (0.69 kb) and F2 (0.689 kb), from 5' and 3' untranslated region (UTR) of the gene were amplified via the primer sets 1762/1763 and 1756/1757, respectively. Fragments F1 and F2 were sequentially cloned into pBC-GFP-hDHFR:yFCU vector at *Xho*I/*Sal*I and *Not*I/*Asc*I sites, respectively. The final construct was then linearized via *Xho*I/*Asc*I and transfected into *P. berghei* ANKA schizonts as previously described in ref. 65. Similarly, the PyMCAT (PY05492) construct was generated by amplifying fragments F3 (0.69 kb) and F4 (0.576 kb) via primer sets 2157/2158 and 2159/2160 and cloned them into pBC-GFP-hDHFR vector at *Xho*I/*Cla*I and *Not*I/*Asc*I, respectively. The construct was linearized via *Xho*I/*Asc*I and transfected into *P.*

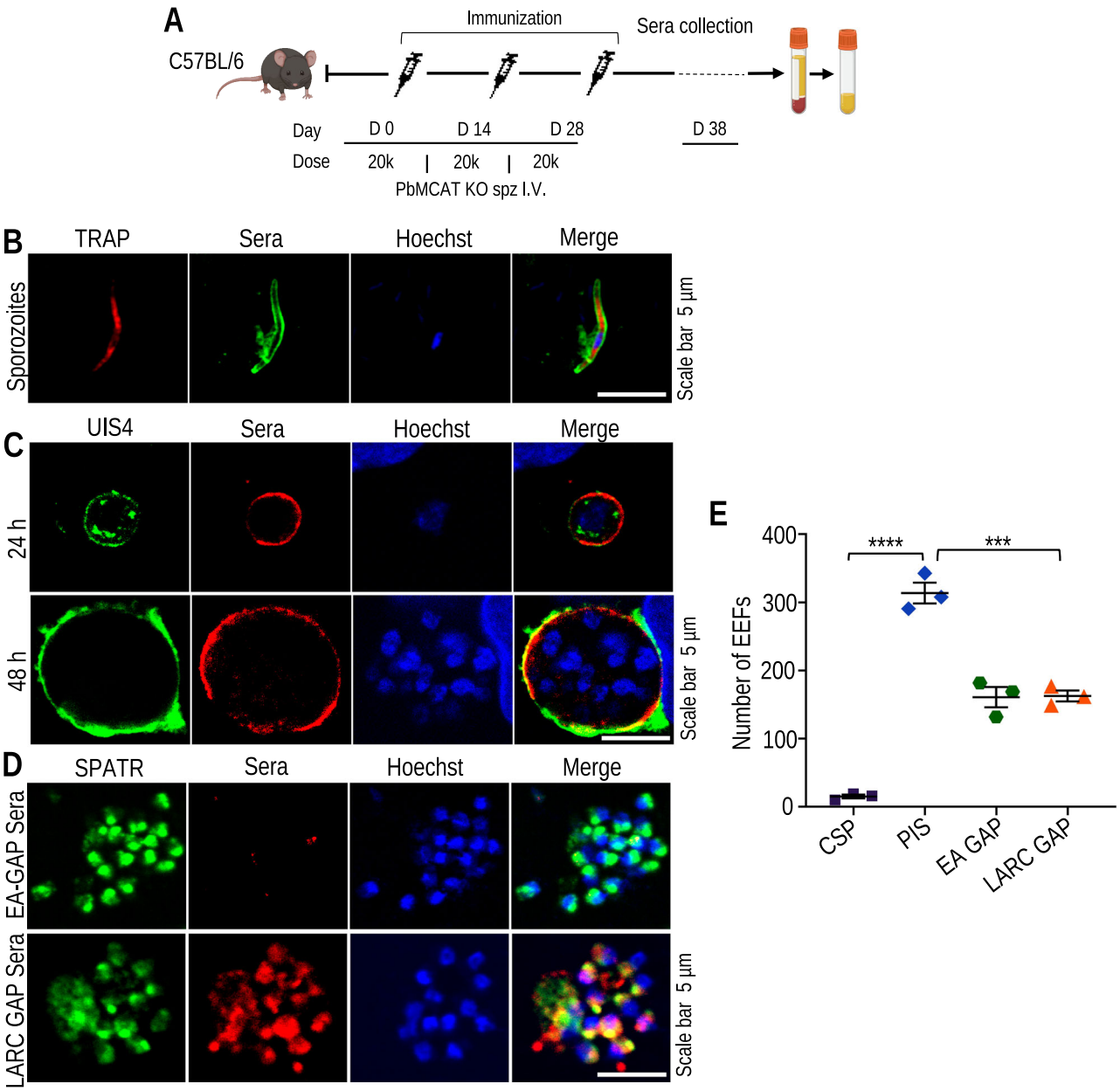

Fig. 7 | Immune sera recognize different stages of the parasite and inhibit the infectivity of sporozoites. A C57BL/6 mice were immunized three times with PbMCAT KO (LARC GAP) sporozoites, and the serum was collected and pooled, as shown in the schematic. **B** Salivary gland sporozoites were immunostained with sera, and an anti-TRAP antibody was used for identification. **C** Immunostaining of EEFs with sera and an anti-UIS4 antibody. **D** Blood-stage schizonts were immunostained with EA-GAP or LARC GAP sera. Parasites were identified using anti-SPATR antibody. LARC GAP sera recognized schizonts, but EA-GAP sera failed to detect them. **E** Preincubation of sporozoites with sera reduced their infectivity. Compared with PIS-incubated sporozoites, there was a significant decrease in the number of EEFs in HepG2 cultures infected with sera-incubated sporozoites (***$P = 0.0003$, one-way ANOVA). The data are shown as the mean ± SEM from three independent experiments performed in duplicate.

yoelii 17XNL schizonts as previously described in ref. 66. The transfected parasites were selected by oral administration of pyrimethamine (Sigma-Aldrich, 46706). Clonal lines were obtained by limiting dilution of the parasites. Correct integration of the targeting cassette was confirmed by diagnostic PCR via primer sets 1866/1225 and 1215/1867 for PbMCAT KO parasites and 2163/1225 and 1215/2164 for PyMCAT KO parasites. PbMCAT complemented parasite line was generated by restoring gene function. For this purpose, a fragment F5 (2.5 kb) comprising 5'UTR, ORF, and 3'UTR of the PbMCAT gene was amplified using primers 1762/1757 and transfected into PbMCAT KO schizonts. The transfected parasites were selected negatively using the drug 5-fluorrocytosine (5-FC) (Sigma-Aldrich, F7129)[67]. The restored PbMCAT locus was confirmed by genotyping using primers 2097/2098. PbMCAT-3XHA-tagged plasmid was obtained from PlasmoGem resources[68,69]. The construct was linearized using *Not*I and transfected into *P. berghei* ANKA schizonts as described above. The correct integration was confirmed via primer pair 2036/2400. Primers used in this study are detailed in Supplementary Table S1.

Western blotting

The purified schizont pellet was resuspended in Laemmli buffer (Bio-Rad, 1610747), resolved via SDS-PAGE and transferred onto a nitrocellulose membrane (Bio-Rad, USA) as previously described in ref. 70. The membrane was blocked with 1% BSA-PBS and further incubated for 1 h at room temperature with anti-HA (dilution 1:1000, C29F4; Cell Signaling

Technology) or anti-HSP70 (dilution 1:1000) antibodies. The membrane was then washed three times with 1X PBST, followed by incubation with HRP-conjugated anti-rabbit or anti-mouse IgG (dilution 1:5000, Amersham Biosciences, United Kingdom, NA934V/NA931V). The membrane was subsequently washed three times with 1X PBST, and the blot was developed using ECL Chemiluminescent Substrate (Bio-Rad, 170-5060) and imaged with a ChemiDoc XRS+ System (Bio-Rad, USA).

Phenotypic characterization of MCAT KO parasites in the blood and mosquito stages

To analyze the asexual blood-stage propagation of MCAT KO parasites, Swiss mice were intravenously injected with an equal number of iRBCs as previously described in ref. 71. The progression of parasitemia was monitored daily via Giemsa-stained blood smears. Female *Anopheles* mosquitoes were allowed to probe for a blood meal on infected mice to initiate parasite transmission in mosquitos. To analyze ookinete development, mosquito midguts were dissected and crushed 24 h after a blood meal and visualized under a fluorescence microscope. Ookinete numbers were quantified using a hemocytometer as previously described in ref. 72. To determine the oocyst numbers and sporogony patterns, the mosquito midguts of *P. yoelii* and *P. berghei* were dissected and imaged on days 9 and 14 post-blood meal, respectively. A batch of mosquito midguts was also crushed with a plunger to enumerate the number of midgut sporozoites. To determine salivary gland sporozoite numbers, *P. yoelii* and *P. berghei* mosquitoes were dissected on days 14-16 and 18-22 post-blood meal, respectively, and the numbers were enumerated as previously described[64].

Analyzing parasite in vivo infection and liver burden

As previously described[55], C57BL/6 mice (5 mice/group) were injected intravenously with salivary gland sporozoites or inoculated via mosquito bites. The appearance of parasites in the blood was monitored by making Giemsa-stained blood smears. To analyze the liver-stage parasite biomass, another group of C57BL/6 mice was inoculated with 5000 salivary gland sporozoites, and the livers were harvested at 40 and 55 hpi. Liver was homogenized in RNAiso Plus (Takara, 9108). The RNA was isolated according to the manufacturer's instructions. cDNA was synthesized as previously described in ref. 73. The parasite burden was quantified by amplifying 18S rRNA via the primers 1195/1196 using real-time PCR (CFX Opus 96 real-time PCR system; Bio-Rad) as previously described in ref. 74. 18S rRNA expression was normalized with amplification of mouse GAPDH using primers 1193/1194. The primers used are listed in Supplementary Table S1.

Analysis of in vitro liver stage development

HepG2 cells were cultured in DMEM supplemented with 10% FBS, and 6×10^4 cells/well were seeded on a 48-well collagen-coated plate. Cells were infected with 5×10^3 sporozoites and fixed with 4% PFA (Sigma-Aldrich, HT5012) at 40 and 55 hpi, as previously described in ref. 75. For the detached cell assay, 1×10^5 HepG2 cells were seeded on a 24-well collagen-coated plate and infected with 3×10^4 sporozoites/well. The culture supernatant was harvested at 65 hpi, and detached cell (merosome) numbers were counted using a hemocytometer. To analyze infectivity, Swiss albino mice were intravenously injected with detached cells, and the appearance of blood-stage infection was monitored by making Giemsa-stained blood smears.

Immunofluorescence assays

Blood and mosquito-stage parasites were prepared and immunostained as previously described in ref. 76. Cells were permeabilized with 0.1% Triton-X-100 (Sigma-Aldrich, T8787) for 10 min at RT. Fixed infected HepG2 culture was permeabilized with Methanol (Merck, SC7SF67273) for 20 min at 4 °C. The permeabilized cells were blocked with 1% BSA/PBS and incubated with primary antibodies for 1–2 h at RT. The following primary antibodies were used: anti-HA (Cell Signaling Technology- C29F4, diluted 1:1000 and 6E2, diluted 1:100), anti-HSP70[77] (diluted 1:1000), anti-CSP[78] (diluted 1:1000), anti-ACP[79] (diluted 1:1000), anti-UIS4[18] (diluted 1:1000), and anti-MSP1[80] (diluted 1:5000). Primary antibody signals were detected via Alexa Fluor 488- or 594-conjugated secondary antibodies as previously described[76] (Invitrogen, diluted 1:1000). Nuclei were stained with Hoechst 33342 (Sigma-Aldrich, 41399). Coverslips were mounted with Prolong Diamond antifade reagent (Invitrogen, P36970). The number of EEFs produced was counted manually, and the area was measured using Nikon NIS elements BR imaging software under an Eclipse 80i fluorescence microscope/Plan Fluor 40x/0.75 objective. Asexual blood-stage and mosquito-stage images were acquired from a Leica DM 3000 LED microscope with 100x (NA 1.25, oil), 40x (NA 0.65, air) or 10x (NA 0.25, air) objectives. Images of EEFs were acquired via FV1000 software on a confocal laser scanning microscope (Olympus BX61WI) with a UPlanSAPO 100x (NA 1.4, oil) objective.

Sporozoite immunization and challenge

P. berghei or *P. yoelii* MCAT KO salivary gland sporozoites were injected intravenously (i.v.) or intramuscularly (i.m.) into C57BL/6 or BALB/c mice, respectively as indicated in schematic. Control mice were injected with salivary gland debris (SGD). Immunized mice were challenged with WT sporozoites 10 to 30 days after the last immunization. Blood stage infection was assessed by making Giemsa-stained blood smears. As previously described, another group of immunized mice was challenged with WT GFP-luciferase-expressing infectious sporozoites[16].

Assessment of immunized mouse serum reactivity

To assess the reactivity of sera against different parasite stages, PbMCAT KO-immunized mice blood was collected in a heparinized tube by retro-orbital bleeding on day 10 post-last immunization. The sera were pooled and used to immunostain sporozoites, EEFs, and iRBCs. Sporozoites, EEFs and iRBCs were immunostained with anti-TRAP, anti-UIS4, and anti-SPATR antibodies to identify the parasites. Nuclei were stained with Hoechst 33342. To check the parasite-neutralizing activity of sera, sporozoites were incubated with sera at 25°C for 20 min and then added to the HepG2 culture as previously described[16]. Cultures were harvested at 36 hpi and immunostained with anti-HSP70 antibody[77]. The number of EEFs was counted under a Leica DM 3000 LED microscope using 40x (NA 0.65, air) objectives.

In vivo imaging of parasite development in the liver

Luciferase activity in the whole bodies of live mice was visualized through imaging as previously described[16]. Briefly, immunized mice were challenged with Pb-GFP-luciferase parasites and then imaged using an in vivo imaging system (IVIS Spectrum) 42–44 h post-challenge. The mice were anesthetized, their belly was shaved, and D-luciferin (100 mg/kg; Promega, P1043) was injected intraperitoneally. Bioluminescence images were acquired with a 10 cm FOV, a medium binning factor, and an exposure time of 120 s. Quantitative bioluminescence analysis was performed by measuring the luminescence signal intensity using the ROI settings of the Aura imaging software. ROI measurements are expressed as total flux (photon/second).

Statistical analysis

Statistical analysis was performed using GraphPad Prism 9 software. The data are presented as the mean ± SEM or mean ± SD. The statistical significance of differences between the two groups was analyzed using an unpaired two-tailed Student's t-test, log-rank Mantel–Cox test, or one-way ANOVA.

Data availability

The data supporting the findings of this study are available within the paper and its supplementary information files. All the datasets and raw data analyzed during the current study will be made available upon request.

Received: 12 November 2024; Accepted: 29 April 2025;
Published online: 16 May 2025

References

1. WHO. *World malaria World malaria report report*, (2023).
2. Fairhurst, R. M. & Dondorp, A. M. Artemisinin-Resistant Plasmodium falciparum Malaria. *Microbiol. Spectr.* **4**, 1–25 (2016).
3. White, N. J. Artemisinin resistance - The clock is ticking. *Lancet* **376**, 2051–2052 (2010).
4. Ogbonna, A. & Uneke, C. J. Artemisinin-based combination therapy for uncomplicated malaria in sub-Saharan Africa: the efficacy, safety, resistance and policy implementation since Abuja 2000. *Trans. R. Soc. Trop. Med. Hyg.* **102**, 621–627 (2008).
5. Zavala, F. RTS,S: the first malaria vaccine. *J. Clin. Invest.* **132**, 1–3 (2022).
6. Datoo, M. S. et al. Efficacy of a low-dose candidate malaria vaccine, R21 in adjuvant Matrix-M, with seasonal administration to children in Burkina Faso: a randomised controlled trial. *Lancet (Lond., Engl.)* **397**, 1809–1818 (2021).
7. El-Moamly, A. A. & El-Sweify, M. A. Malaria vaccines: the 60-year journey of hope and final success—lessons learned and future prospects. *Trop. Med. Health* **51**, (2023).
8. Nussenzweig, R. S., Vanderberg, J., Most, H. & Orton, C. Protective immunity produced by the injection of x-irradiated sporozoites of plasmodium berghei. *Nature* **216**, 160–162 (1967).
9. Oakley, M. S. et al. Molecular Markers of Radiation Induced Attenuation in Intrahepatic Plasmodium falciparum Parasites. *PLoS One* **11**, e0166814 (2016).
10. Richie, T. L. et al. Sporozoite immunization: innovative translational science to support the fight against malaria. *Expert Rev. Vaccines* **22**, 964–1007 (2023).
11. Mordmüller, B. et al. Sterile protection against human malaria by chemoattenuated PfSPZ vaccine. *Nature* **542**, 445–449 (2017).
12. Mwakingwe-Omari, A. et al. Two chemoattenuated PfSPZ malaria vaccines induce sterile hepatic immunity. *Nature* **595**, 289–294 (2021).
13. Moita, D. et al. Variable long-term protection by radiation-, chemo-, and genetically-attenuated Plasmodium berghei sporozoite vaccines. *Vaccine* **41**, 7618–7625 (2023).
14. Nunes-Cabaço, H., Moita, D. & Prudêncio, M. Five decades of clinical assessment of whole-sporozoite malaria vaccines. *Front. Immunol.* **13**, 977472 (2022).
15. Goswami, D. et al. A replication competent Plasmodium falciparum parasite completely attenuated by dual gene deletion. *EMBO Mol. Med.* **16**, 723–754 (2024).
16. Mishra, A., Paul, P., Srivastava, M. & Mishra, S. A Plasmodium late liver stage arresting GAP provides superior protection in mice. *npj Vaccines* **9**, 1–15 (2024).
17. Mueller, A.-K., Labaied, M., Kappe, S. H. I. & Matuschewski, K. Genetically modified Plasmodium parasites as a protective experimental malaria vaccine. *Nature* **433**, 164–167 (2005).
18. Mueller, A. K. et al. Plasmodium liver stage developmental arrest by depletion of a protein at the parasite-host interface. *Proc. Natl Acad. Sci. USA* **102**, 3022–3027 (2005).
19. Jobe, O. et al. Genetically attenuated Plasmodium berghei liver stages induce sterile protracted protection that is mediated by major histocompatibility complex Class I-dependent interferon-gamma-producing CD8+ T cells. *J. Infect. Dis.* **196**, 599–607 (2007).
20. van Schaijk, B. C. L. et al. A genetically attenuated malaria vaccine candidate based on P. falciparum b9/slarp gene-deficient sporozoites. *Elife* **3**, (2014).
21. Murphy, S. C. et al. A genetically engineered Plasmodium falciparum parasite vaccine provides protection from controlled human malaria infection. *Sci. Transl. Med.* **14**, eabn9709 (2022).
22. Mikolajczak, S. A. et al. A next-generation genetically attenuated Plasmodium falciparum parasite created by triple gene deletion. *Mol. Ther.* **22**, 1707–1715 (2014).
23. Roestenberg, M. et al. A double-blind, placebo-controlled phase 1/2a trial of the genetically attenuated malaria vaccine PfSPZ-GA1. *Sci. Transl. Med.* **12**, 1–9 (2020).
24. Dankwa, D. A., Davis, M. J., Kappe, S. H. I. & Vaughan, A. M. A Plasmodium yoelii Mei2-like RNA binding protein is essential for completion of liver stage schizogony. *Infect. Immun.* **84**, 1336–1345 (2016).
25. Goswami, D. et al. A replication-competent late liver stage–attenuated human malaria parasite. *JCI Insight* **5**, 1–19 (2020).
26. Franke-Fayard, B. et al. Creation and preclinical evaluation of genetically attenuated malaria parasites arresting growth late in the liver. *NPJ vaccines* **7**, 139 (2022).
27. Roozen, G. V. T. et al. Single immunization with genetically attenuated PfΔmei2 (GA2) parasites by mosquito bite in controlled human malaria infection: a placebo-controlled randomized trial. *Nat. Med.* **31**, 218–222 (2025).
28. Moita, D. & Prudêncio, M. Whole-sporozoite malaria vaccines: where we are, where we are going. *EMBO Mol. Med.* **16**, 2279–2289 (2024).
29. Mendes, A. M. et al. A Plasmodium berghei sporozoite-based vaccination platform against human malaria. *NPJ vaccines* **3**, 33 (2018).
30. Reuling, I. J. et al. An open-label phase 1/2a trial of a genetically modified rodent malaria parasite for immunization against Plasmodium falciparum malaria. *Sci. Transl. Med*. **12**, 1-12 (2020).
31. Moita, D. et al. A genetically modified Plasmodium berghei parasite as a surrogate for whole-sporozoite vaccination against P. vivax malaria. *NPJ vaccines* **7**, 163 (2022).
32. Pei, Y. et al. Plasmodium pyruvate dehydrogenase activity is only essential for the parasite's progression from liver infection to blood infection. *Mol. Microbiol.* **75**, 957–971 (2010).
33. Vaughan, A. M. et al. Type II fatty acid synthesis is essential only for malaria parasite late liver stage development. *Cell. Microbiol.* **11**, 506–520 (2009).
34. Yu, M. et al. The fatty acid biosynthesis enzyme FabI plays a key role in the development of liver-stage malarial parasites. *Cell Host Microbe* **4**, 567–578 (2008).
35. Annoura, T. et al. Assessing the adequacy of attenuation of genetically modified malaria parasite vaccine candidates. *Vaccine* **30**, 2662–2670 (2012).
36. Butler, N. S. et al. Superior antimalarial immunity after vaccination with late liver stage-arresting genetically attenuated parasites. *Cell Host Microbe* **9**, 451–462 (2011).
37. Keitany, G. J. et al. Immunization of mice with live-attenuated late liver stage-arresting plasmodium yoelii parasites generates protective antibody responses to preerythrocytic stages of malaria. *Infect. Immun.* **82**, 5143–5153 (2014).
38. van Schaijk, B. C. L. et al. Type II fatty acid biosynthesis is essential for Plasmodium falciparum sporozoite development in the midgut of Anopheles mosquitoes. *Eukaryot. Cell* **13**, 550–559 (2014).
39. Verwoert, I. I. G. S., Verbree, E. C., Van der Linden, K. H., Nijkamp, H. J. J. & Stuitje, A. R. Cloning, nucleotide sequence, and expression of the Escherichia coli fabD gene, encoding malonyl coenzyme A-acyl carrier protein transacylase. *J. Bacteriol.* **174**, 2851–2857 (1992).
40. Prigge, S. T., He, X., Gerena, L., Waters, N. C. & Reynolds, K. A. The initiating steps of a type II fatty acid synthase in Plasmodium falciparum are catalyzed by pfACP, pfMCAT, and pfKASIII. *Biochemistry* **42**, 1160–1169 (2003).
41. Nganou-Makamdop, K. & Sauerwein, R. W. Liver or blood-stage arrest during malaria sporozoite immunization: the later the better? *Trends Parasitol.* **29**, 304–310 (2013).
42. Waller, R. F. et al. Nuclear-encoded proteins target to the plastid in Toxoplasma gondii and Plasmodium falciparum. *Proc. Natl. Acad. Sci. USA* **95**, 12352–12357 (1998).
43. Labaied, M. et al. Plasmodium yoelii sporozoites with simultaneous deletion of P52 and P36 are completely attenuated and confer sterile immunity against infection. *Infect. Immun.* **75**, 3758–3768 (2007).
44. VanBuskirk, K. M. et al. Preerythrocytic, live-attenuated Plasmodium falciparum vaccine candidates by design. *Proc. Natl. Acad. Sci. USA* **106**, 13004–13009 (2009).

45. Nagel, A. et al. A new approach to generate a safe double-attenuated Plasmodium liver stage vaccine. *Int. J. Parasitol.* **43**, 503–514 (2013).
46. Goswami, D., Minkah, N. K. & Kappe, S. H. I. Designer Parasites: Genetically Engineered Plasmodium as Vaccines To Prevent Malaria Infection. *J. Immunol.* **202**, 20–28 (2019).
47. Moita, D. & Prudêncio, M. A new malaria vaccination tool based on replication-competent Plasmodium falciparum parasites. *EMBO Mol. Med.* **16**, 667–669 (2024).
48. Hafalla, J. C. R., Borrmann, S. & Matuschewski, K. Genetically attenuated parasites show promise as a next-generation malaria vaccine. *Trends Parasitol.* **41**, 75–77 (2025).
49. Vaughan, A. M. et al. A Plasmodium parasite with complete late liver stage arrest protects against preerythrocytic and erythrocytic stage infection in mice. *Infect. Immun.* **86**, 1–18 (2018).
50. Goswami, D. et al. A conserved Plasmodium nuclear protein is critical for late liver stage development. *Commun. Biol.* **7**, 1387 (2024).
51. Sissoko, M. S. et al. Safety and efficacy of PfSPZ Vaccine against Plasmodium falciparum via direct venous inoculation in healthy malaria-exposed adults in Mali: a randomised, double-blind phase 1 trial. *Lancet Infect. Dis.* **17**, 498–509 (2017).
52. Seder, R. A. et al. Protection against malaria by intravenous immunization with a nonreplicating sporozoite vaccine. *Science* **341**, 1359–1365 (2013).
53. Mi-Ichi, F., Kita, K. & Mitamura, T. Intraerythrocytic Plasmodium falciparum utilize a broad range of serum-derived fatty acids with limited modification for their growth. *Parasitology* **133**, 399–410 (2006).
54. Krishnegowda, G. & Gowda, D. C. Intraerythrocytic Plasmodium falciparum incorporates extraneous fatty acids to its lipids without any structural modification. *Mol. Biochem. Parasitol.* **132**, 55–58 (2003).
55. Ghosh, A. et al. A Micronemal Protein, Scot1, Is Essential for Apicoplast Biogenesis and Liver Stage Development in Plasmodium berghei. *ACS Infect. Dis.* **10**, 3013–3025 (2024).
56. van Dijk, M. R. et al. Genetically attenuated, P36p-deficient malarial sporozoites induce protective immunity and apoptosis of infected liver cells. *Proc. Natl. Acad. Sci. USA* **102**, 12194–12199 (2005).
57. Ishino, T., Chinzei, Y. & Yuda, M. A Plasmodium sporozoite protein with a membrane attack complex domain is required for breaching the liver sinusoidal cell layer prior to hepatocyte infection. *Cell. Microbiol.* **7**, 199–208 (2005).
58. M'Bana, V., Lahree, A., Marques, S., Slavic, K. & Mota, M. M. Plasmodium parasitophorous vacuole membrane-resident protein UIS4 manipulates host cell actin to avoid parasite elimination. *iScience* **25**, 104281 (2022).
59. Ralph, S. A. et al. Tropical infectious diseases: metabolic maps and functions of the Plasmodium falciparum apicoplast. *Nat. Rev. Microbiol.* **2**, 203–216 (2004).
60. Ramakrishnan, S., Serricchio, M., Striepen, B. & Bütikofer, P. Lipid synthesis in protozoan parasites: a comparison between kinetoplastids and apicomplexans. *Prog. Lipid Res.* **52**, 488–512 (2013).
61. Roques, M., Bindschedler, A., Beyeler, R. & Heussler, V. T. Same, same but different: Exploring Plasmodium cell division during liver stage development. *PLoS Pathog.* **19**, 1–22 (2023).
62. Spring, M. et al. First-in-human evaluation of genetically attenuated Plasmodium falciparum sporozoites administered by bite of Anopheles mosquitoes to adult volunteers. *Vaccine* **31**, 4975–4983 (2013).
63. Sedegah, M., Weiss, W. W. & Hoffman, S. L. Cross-protection between attenuated Plasmodium berghei and P. yoelii sporozoites. *Parasite Immunol.* **29**, 559–565 (2007).
64. Narwal, S. K. et al. Stearoyl-CoA desaturase regulates organelle biogenesis and hepatic merozoite formation in Plasmodium berghei. *Mol. Microbiol*. https://doi.org/10.1111/mmi.15246 (2024).
65. Janse, C. J., Ramesar, J. & Waters, A. P. High-efficiency transfection and drug selection of genetically transformed blood stages of the rodent malaria parasite Plasmodium berghei. *Nat. Protoc.* **1**, 346–356 (2006).
66. Mota, M. M., Thathy, V., Nussenzweig, R. S. & Nussenzweig, V. Gene targeting in the rodent malaria parasite Plasmodium yoelii. *Mol. Biochem. Parasitol.* **113**, 271–278 (2001).
67. Lin, J. W. et al. A novel 'Gene Insertion/Marker Out' (GIMO) method for transgene expression and gene complementation in rodent malaria parasites. *PLoS One* **6**, 1-13 (2011).
68. Gomes, A. R. et al. A genome-scale vector resource enables high-throughput reverse genetic screening in a malaria parasite. *Cell Host Microbe* **17**, 404–413 (2015).
69. Godiska, R. et al. Linear plasmid vector for cloning of repetitive or unstable sequences in Escherichia coli. *Nucleic Acids Res.* **38**, e88 (2010).
70. Mishra, A., Varshney, A. & Mishra, S. Regulation of Atg8 membrane deconjugation by cysteine proteases in the malaria parasite Plasmodium berghei. *Cell. Mol. Life Sci*. **80**, 1-20 (2023).
71. Ghosh, A. et al. The novel Plasmodium berghei protein S14 is essential for sporozoite gliding motility and infectivity. *J. Cell Sci*. **137**, 1-11 (2024).
72. Nayak, B., Paul, P. & Mishra, S. Neddylation is essential for malaria transmission in Plasmodium berghei. *MBio* e0023224 https://doi.org/10.1128/mbio.00232-24 (2024).
73. Choudhary, H. H., Gupta, R. & Mishra, S. PKAc is not required for the preerythrocytic stages of Plasmodium berghei. *Life Science Alliance* **2**, 1–11 (2019).
74. Bruna-Romero, O. et al. Detection of malaria liver-stages in mice infected through the bite of a single Anopheles mosquito using a highly sensitive real-time PCR. *Int. J. Parasitol.* **31**, 1499–1502 (2001).
75. Mishra, A., Srivastava, P. N., H, S. A. & Mishra, S. Autophagy protein Atg7 is essential and druggable for maintaining malaria parasite cellular homeostasis and organelle biogenesis. at https://doi.org/10.1101/2023.08.16.553492 (2023).
76. Narwal, S. K., Nayak, B., Mehra, P. & Mishra, S. Protein kinase 9 is not required for completion of the Plasmodium berghei life cycle. *Microbiol. Res.* **260**, 127051 (2022).
77. Tsuji, M., Mombaertst, P., Lefrancoist, L. E. O., Nussenzweig, R. S. & Zavala, F. *γδ T cells contribute Immun. liver stages Malar. c43 T-cell-deficient mice* **91**, 345–349 (1994).
78. Yoshida, N., Nussenzweig, R. S., Potocnjak, P., Nussenzweig, V. & Aikawa, M. Hybridoma produces protective antibodies directed against the sporozoite stage of malaria parasite. *Sci. (80-.)* **207**, 71–73 (1980).
79. Gallagher, J. R. & Prigge, S. T. Plasmodium falciparum acyl carrier protein crystal structures in disulfide-linked and reduced states and their prevalence during blood stage growth. *Proteins* **78**, 575–588 (2010).
80. Holder, A. A. & Freeman, R. R. Immunization against blood-stage rodent malaria using purified parasite antigens. *Nature* **294**, 361–364 (1981).

Acknowledgements

We thank BEI Resources, USA, for the parasite strains and plasmids. We acknowledge Sanger as having made available the Materials and Lucigen as the source of the plasmid vector used to generate the PlasmoGEM resource. We thank Dr. Anthony A. Holder (The Francis Crick Institute, UK), Drs. Photini Sinnis and Sean Prigge (Johns Hopkins University, USA) for anti-MSP1, anti-UIS4, and anti-ACP antibodies, respectively. We also thank Dr. V.A. Nagaraj for the modified version of the GOMO-GFP-Luc plasmid originally obtained from Addgene (#60976) deposited by Dr. Olivier Silvie for generating *P. berghei* Luc parasites. We acknowledge the CSIR-CDRI's Intravital microscopy facility. The University Grants Commission, Government of India research fellowship supported RD. This study was supported by a CSIR-CDRI Inhouse project (IHP0030) and an Anusandhan National Research

Foundation grant (CRG/2022/003848) to SM. The graphics were created with Biorender.com. This manuscript is CDRI communication no. 10982.

Author contributions

Conception and design of study: R.D., S.M.; Acquisition of data: R.D., R.N., S.M.; Analysis of data: R.D., S.M.; Drafting and revisions of the Manuscript: R.D., S.M. All authors have read and approved the final version of the manuscript.

Competing interests

The authors declare no competing interests.

Additional information

Supplementary information The online version contains supplementary material available at https://doi.org/10.1038/s41541-025-01149-2.

Correspondence and requests for materials should be addressed to Satish Mishra.